J. Biochem. **135**, 421–427 (2004)
DOI: 10.1093/jb/mvh050

Inhibitory Effect of 0.19 α-Amylase Inhibitor from Wheat Kernel on the Activity of Porcine Pancreas α-Amylase and Its Thermal Stability

Hiroshi Oneda, Seungjae Lee and Kuniyo Inouye*

Division of Food Science and Biotechnology, Graduate School of Agriculture, Kyoto University, Sakyo-ku, Kyoto 606-8502

Received December 2, 2003; accepted January 26, 2004

The inhibitory effect of 0.19 α-amylase inhibitor (0.19 AI) from wheat kernel on the porcine pancreas α-amylase (PPA)–catalyzed hydrolysis of *p*-nitrophenyl-α-D-maltoside (*p*NP-G2) was examined. 0.19 AI is a homodimer of 26.6 kDa with 13.3-kDa subunits under the conditions used. The elution behaviors in gel filtration HPLC of PPA and 0.19 AI indicated that a PPA molecule bound with a 0.19 AI molecule (homodimer) at a molar ratio of 1:1. 0.19 AI inhibited PPA activity in a competitive manner with an inhibitor constant, K_i, of 57.3 nM at pH 6.9, 30°C, and the binding between them was found to be endothermic and entropy-driven. The activation energy for the thermal inactivation of 0.19 AI was determined to be 87.0 kJ/mol, and the temperature, T_{50}, giving 50% inactivation in a 30-min incubation at pH 6.9 was 88.1°C. The high inhibitory activity of 0.19 AI against PPA and its high thermal stability suggest its potential for use in the prevention and therapy of obesity and diabetes.

Key words: α-amylase inhibitor, proteinaceous inhbitor, thermostability, wheat kernel.

Abbreviations: AI, α-amylase inhibitor; *p*NP-G2, *p*-nitrophenyl-α-D-maltoside; PPA, porcine pancreas α-amylase.

Plants contain a large number of inhibitors against amylases and proteinases. They are present in seeds and vegetative organs and are believed to function in resistance against predation by phytophagous insects (*1*).

Wheat (*Triticum aestivum*) kernel contains a number of proteinaceous α-amylase inhibitors (AIs), which are by-products of starch and gluten manufacture. Recently, interest in wheat AIs has focused on their therapeutic effects on obesity and non-insulin-dependent diabetes. They are reported to delay postprandial carbohydrate digestion and absorption, and lower plasma glucose levels without altering pancreatic growth (*2–4*). These observations strongly suggest that these untapped proteinaceous resources may be applicable to the therapy of obesity and diabetes.

Wheat AIs are classified into three families of 60, 24, and 12 kDa (*5*). The 60-kDa family members exist as heterotetramers composed of CM proteins (*6*). The 12-kDa family members, including 0.28 AI, designated according to its electrophoretic mobility on a native gel (*7*, *8*), exist as monomers (*9*). The 24-kDa family members, including 0.19, 0.36, 0.38, and 0.53 AIs exist as dimers (*2*).

0.19 AI of the 24-kDa family is the major component of wheat AIs. It inhibits α-amylases from *Bacillus subtilis* (*10*), yellow mealworm (*11*), cowpea weevil, Mexican bean weevil, bean weevil, porcine pancreas (*12*), chicken pancreas (*13*), and human saliva (*2*, *14*) and pancreas (*2*). 0.19 AI is a homodimer of molecular weight 26,600, comprising two identical 13.3-kDa subunits composed of 124 amino acid residues that are associated by non-covalent interactions (*15*). The X-ray crystallographic analysis of 0.19 AI demonstrated that each subunit is composed of four major α-helices, one one-turn helix, and two short antiparalell β-strands. The subunits in a dimer are related each other by non-crystallographic 2-fold axis, and the interface is mainly composed of hydrophobic residues (*16*). Although 0.19 AI has been extensively studied with respect to its structure, properties, and inhibitory activity (*17–19*), little is known about its interaction with amylase, including the amylase-binding site and the inhibition mechanism.

The objective of this paper is to provide some insights into the inhibitory effect of 0.19 AI on porcine pancreas α-amylase isomer-I (PPA) kinetically as well as its thermal stability. It was found that a PPA molecule (E) binds a 0.19 AI homodimer (I_2) to form the EI_2 complex, and that the inhibition of I_2 against E is competitive.

MATERIALS AND METHODS

Materials—Pancreatin (Lot 57F-0658) was purchased from Sigma (St. Louis, MO). A crude preparation of wheat α-amylase inhibitor containing 0.19, 0.28, 0.36, 0.38, 0.53, and other AIs, which was prepared according to the method reported previously (*2*), was a generous gift from Nagata Sangyo (Hyogo). All other chemicals were of reagent grade and purchased from Nacalai Tesque (Kyoto).

Purification of PPA—One gram of pancreatin was dissolved in 100 ml of 15 mM Tris-HCl buffer (pH 8.3) (buffer A). Sixty-seven milliliters of chilled acetone was added to the solution, followed by centrifugation at 10,000 ×*g* for 30 min. Acetone was further added to the supernatant to a final concentration of 67%, and the precipitates were collected by centrifugation. The precipitates were then dissolved in buffer A and applied to anion-exchange HPLC on a TSKgel Super Q-5PW column [7.5 mm (inner diameter) × 75 mm] (Tosoh, Tokyo) equili-

*To whom correspondence should be addressed. Tel: +81-75-753-6266, Fax: +81-75-753-6265, E-mail: inouye@kais.kyoto-u.ac.jp

brated with the same buffer. A linear gradient was generated from 0 M to 50 mM NaCl at time 5 min over 25 min at a flow-rate of 1 ml/min at 25°C. PPA-I and PPA-II were eluted at 19.2 and 25.4 mM NaCl, respectively, and the former was collected for further analysis. Hereafter, PPA-I is abbreviated as PPA. The concentration of PPA was determined spectrophotometrically by using the molar absorption coefficient at 280 nm of 1.28×10^5 M^{-1} cm^{-1} calculated from the amino acid composition (*20*). Absorption was measured with a Shimadzu UV-2200 spectrophotometer (Kyoto).

Purification of 0.19 AI—One gram of crude AI was dissolved in 100 ml of 15 mM borate buffer (pH 10.0) (7.9 mg protein/ml) and dialyzed against the same buffer. Fifty microliters of the solution was then applied to anion-exchange HPLC on a TSKgel BioAssist Q column [10 mm (inner diameter) × 50 mm] (Tosoh) equilibrated with the same buffer. Wheat AIs were separated over 130 min at a flow-rate of 80 μl/min at 25°C. 0.19 AI was eluted at around 75 min, and the fraction eluted from 70 min to 80 min was collected for further analyses. The concentration of 0.19 AI was determined by using the molar absorption coefficient at 280 nm of 34,200 M^{-1} cm^{-1} calculated from the amino acid composition (*15*).

Polyacrylamide Gel Electrophoresis (PAGE)—Native PAGE was performed in a 7.5% gel system, and SDS-PAGE was performed in a 15–25% gradient gel system (PAG mini Daiichi, Lot 124RCA, Daiichi Pure Chemicals, Tokyo) under non-reducing conditions according to the method of Laemmli (*21*). A constant current of 40 mA was applied, and proteins were stained with Coomassie Brilliant Blue R-250. A molecular weight marker kit consisting horse muscle myoglobin II (6.2 kDa), I (8.2 kDa), I and III (10.7 kDa), I and II (14.4 kDa), myoglobin (17.0 kDa), hen eggwhite lysozyme (14.4 kDa), soybean trypsin inhibitor (20.1 kDa), bovine erythrocyte carbonic anhydrase (30.0 kDa), rabbit muscle aldolase (42.4 kDa), bovine serum albumin (66.3 kDa), and rabbit muscle phosphorylase *b* (97.4 kDa) was a product of Daiichi Pure Chemicals.

Gel-Filtration High-Performance Liquid Chromatography (HPLC)—Gel filtration HPLC was performed on a TSKgel G2000SW_{XL} column [7.8 mm (inner diameter) × 30 cm] (Tosoh) equilibrated with 20 mM sodium phosphate buffer, pH 6.9 (buffer B) containing 0.3 M NaCl at a flow-rate of 1.0 ml/min at 30°C. PPA and 0.19 AI were incubated in buffer B containing 25 mM NaCl at 30°C for 30 min, and 200 μl of the mixture was then applied to HPLC. Molecular weight markers used were horse heart cytochrome c (12.4 kDa), horse muscle myoglobin (17.2 kDa), bovine erythrocyte carbonic anhydrase (30.0 kDa), hen eggwhite albumin (45.0 kDa), and bovine serum albumin (66.3 kDa).

PPA-Catalyzed Hydrolysis of pNP-G2—It is known that *p*NP-G2 is hydrolyzed by PPA at one position to produce *p*-nitrophenol (*p*NP) (*22*). PPA-catalyzed hydrolysis of *p*NP-G2 was measured in buffer B (pH 6.9) containing 25 mM NaCl, by following the increase in absorbance at 400 nm due to *p*NP. The amount of *p*NP produced was determined by using the molar absorption coefficient of 9,470 M^{-1} cm^{-1} at pH 6.9 (*23*). The kinetic parameters, the catalytic constant (k_{cat}) and Michaelis constant (K_m), were determined by using the linear least-squares method.

Inhibition of PPA by 0.19 AI—PPA was incubated with 0.19 AI in buffer B for 30 min at a temperature of 20–40°C. The hydrolysis was then initiated by adding *p*NP-G2 to the reaction mixture. The initial concentrations of PPA, 0.19 AI, and *p*NP-G2 were 165 nM, 0–457 nM, and 4.0 mM, respectively. The standard enthalpy change ($\Delta H^{\circ\prime}$) for the binding of PPA with 0.19 AI was determined from the slope ($\Delta H^{\circ\prime}/R$) of the plot of ln K_i against $1/T$ (Van't Hoff plots). The standard Gibbs energy change $\Delta G^{\circ\prime}$ and the standard entropy change $\Delta S^{\circ\prime}$ for the binding of PPA with 0.19 AI were determined according to the following equations (*24*):

$$\Delta G^{\circ\prime} = -RT \ln \frac{1}{K_i} \quad (1)$$

$$\Delta S^{\circ\prime} = \frac{\Delta H^{\circ\prime} - \Delta G^{\circ\prime}}{T} \quad (2)$$

Thermal Inactivation of 0.19 AI—0.19 AI was incubated in buffer B containing 25 mM NaCl for a specified period at a temperature of 50–90°C, followed by mixing with PPA. The 0.19 AI-PPA reaction mixture was further incubated at pH 6.9, 30°C, for 30 min, and then the enzyme activity was measured with *p*NP-G2. The initial concentrations of PPA, 0.19 AI, and *p*NP-G2 in the reaction mixture were 165 nM, 100 nM, and 4.0 mM, respectively. The concentration of the active or free 0.19 AI was calculated from the residual inhibitory activity, and the K_i value at pH 6.9, 30°C. The apparent first-order rate constant (k) of the thermal inactivation was determined by fitting to the following equation:

$$\frac{[I_2]}{[I_2]_o} = e^{-k \cdot t} \quad (3)$$

where $[I_2]_o$ and $[I_2]$ are the initial and active concentrations of 0.19 AI (homodimer), respectively. The activation energy (E_a) for the thermal inactivation was determined from the slope of the Arrhenius plots of k against $1/T$, and the Gibbs energy of activation $\Delta G^{\ddagger}$, the enthalpy of activation $\Delta H^{\ddagger}$, and the entropy of activation $\Delta S^{\ddagger}$ were determined according to the following equations (*24*, *25*):

$$\Delta G^{\ddagger} = -RT\left(\ln \frac{hk}{k_B T}\right) \quad (4)$$

$$\ln \frac{hk}{k_B T} = \frac{\Delta H^{\ddagger}}{RT} + \frac{\Delta S^{\ddagger}}{R} \quad (5)$$

where kB, h, and R are the Boltzman, Plank, and gas constants, respectively, and T is the temperature shown in the Kelvin unit.

RESULTS

Purification of 0.19 AI—Figure 1A shows an elution pattern of the crude wheat AI on an anion-exchange HPLC column, TSKgel BioAssist Q. By means of the isocratic elution at a considerably low flow-rate of 80 μl/min, wheat AIs were successfully separated, and the fraction eluted from 70 to 80 min was collected. The purity of the preparation was also confirmed by PAGE (Fig. 1B). The preparation showed a single band corresponding to 13.3 kDa on the SDS-PAGE and a single band on the native

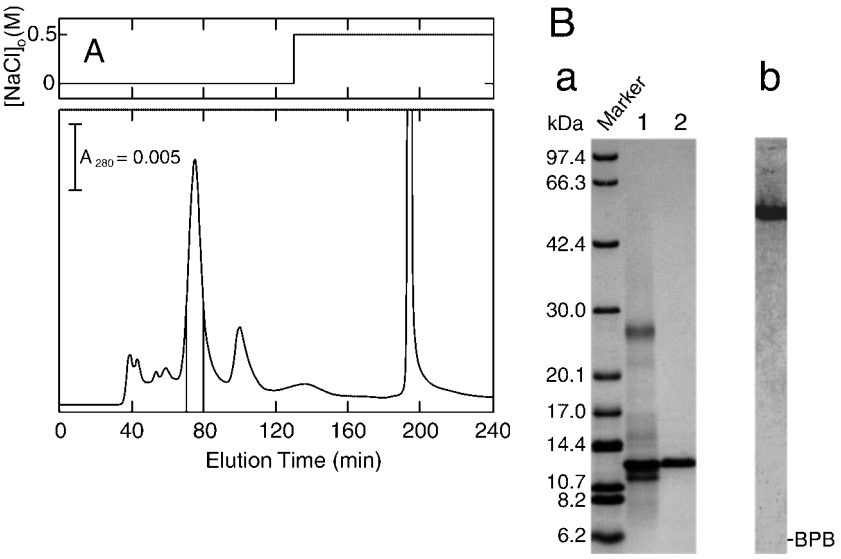

Fig. 1. **Purification of 0.19 AI by anion-exchange HPLC with TSKgel BioAssist Q.** Panel A: Separation of crude AI. A 7.9 mg/ml solution of crude AI was dialyzed against 15 mM borate buffer (pH 10.0), and 50 μl of the solution (containing 0.40 mg) was subjected to the column equilibrated with the same buffer. The elution was monitored by absorbance at 280 nm. The flow-rate was 80 μl/min. The fraction eluted from 70 to 80 min was collected, and it was shown that 0.16 mg protein was purified in this fraction. Panel B: Polyacrylamide gel electrophoresis of the preparation. a: SDS-PAGE was performed in a 15–25% gradient-gel system. Lane 1, crude AI containing 7.9 μg protein. Lane 2, the purified preparation containing 1.8 μg protein. b: Native PAGE was performed in a 7.5% gel system, and the preparation of 1.8 μg was applied to the lane. The relative electrophoretic mobility of the preparation was determined to be 0.19 by comparing the mobility of the preparation with that of bromophenol blue.

PAGE with a mobility of 0.19 with respect to that of bromophenol blue (BPB). By this procedure, 1.3 mg of 0.19 AI was purified to homogeneity from 3.2 mg of crude AI.

HPLC Analysis of the Complex Formation—The elution behaviors of PPA, 0.19 AI, and the complex in a gel filtration HPLC column, TSKgel G2000SW$_{XL}$ are shown in Fig. 2. Under these conditions, PPA was eluted at 10.2 min. The molecular mass of PPA was evaluated to be 17 kDa from this elution time, although its true molecular mass was 55.4 kDa. On the other hand, 0.19 AI was eluted at 9.5 min, suggesting that its molecular mass could be 24.0 kDa. When PPA (E) and 0.19 AI (dimer, I_2) were incubated at a molar ratio of 1:1, a new peak was appeared at 8.7 min, which suggests that the molecular mass of the protein in the peak might be 35.0 kDa. When E and I_2 were incubated at a molar ratio of 2:1, no new peaks appeared, and the peak of the excess of free PPA was observed at 10.2 min. These elution profiles clearly indicated that E bound with I_2 at a molar ratio of 1:1 to form EI_2 complex, and E_2I_2 complex was not formed, although 0.19 AI existed as a homodimer.

Competitive Inhibition of PPA activity by 0.19 AI—Figure 3 shows the Hanes-Woolf plots for the hydrolysis of *p*NP-G2 at pH 6.9 and 30°C. The catalytic constant (k_{cat}) and Michaelis constant (K_m) for the hydrolysis of *p*NP-G2 at pH 6.9 and 30°C were determined to be (5.23 ± 0.21) × 10^{-2} s^{-1} and 4.17 ± 0.35 mM, respectively. A line

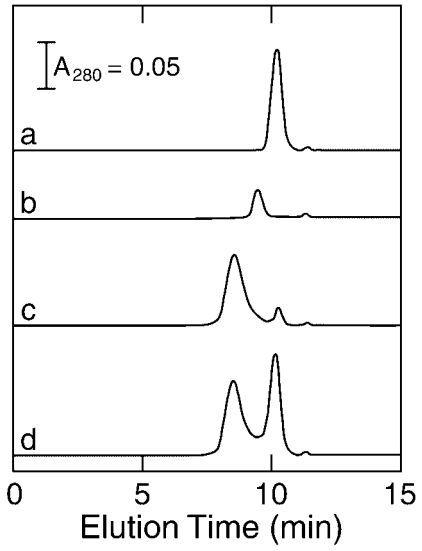

Fig. 2. **HPLC analysis of the complex formation.** 0.19 AI dimer (I_2; 1.45 μM) was incubated with PPA in buffer B (pH 6.9) containing 25 mM NaCl for 30 min. Two hundred μl of the mixture was then subjected to a TSKgel G2000SW$_{XL}$ column equilibrated with buffer B containing 0.3 M NaCl. The molar ratios of PPA (E) : 0.19 AI dimer (I_2) are (a) 0 : 1, (b) 1 : 0, (c) 1 : 1, and (d) 2 : 1. Accordingly, the composition of the mixtures are (a) 1.45 μM I_2; (b) 1.45 μM E; (c) 1.45 μM E + 1.45 μM I_2; and (d) 2.90 μM E + 1.45 μM I_2.

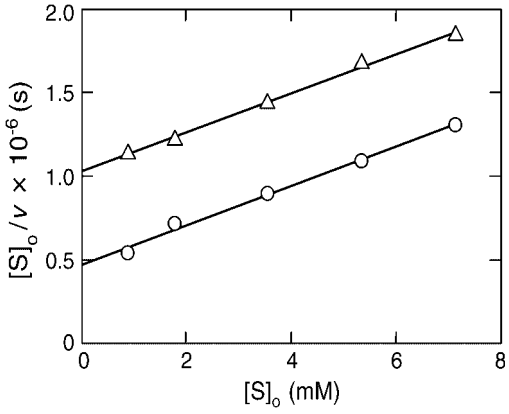

Fig. 3. **Hanes-Woolf plots for the hydrolysis of *p*NP-G2.** PPA was incubated with 0 M (circles) and 117 nM 0.19 AI (triangles) in buffer B, pH 6.9, containing 25 mM NaCl. The reaction was initiated by adding substrate *p*NP-G2 to the reaction mixture. The initial concentration of PPA ($[E]_o$) was 182 nM, and that of 0.19 AI ($[I_2]_o$) was 0 or 117 nM. The initial concentrations of substrate ($[S]_o$) were in the range of 0.9 mM to 7.2 mM. The catalytic constant (k_{cat}) and Michaelis constant (K_m) in the absence of 0.19 AI were determined to be (5.23 ± 0.21) × 10^{-2} s^{-1} and 4.17 ± 0.35 mM, and those in the presence of 117 nM 0.19 AI were (5.25 ± 0.21) × 10^{-2} s^{-1} and 8.93 ± 0.55 mM, respectively.

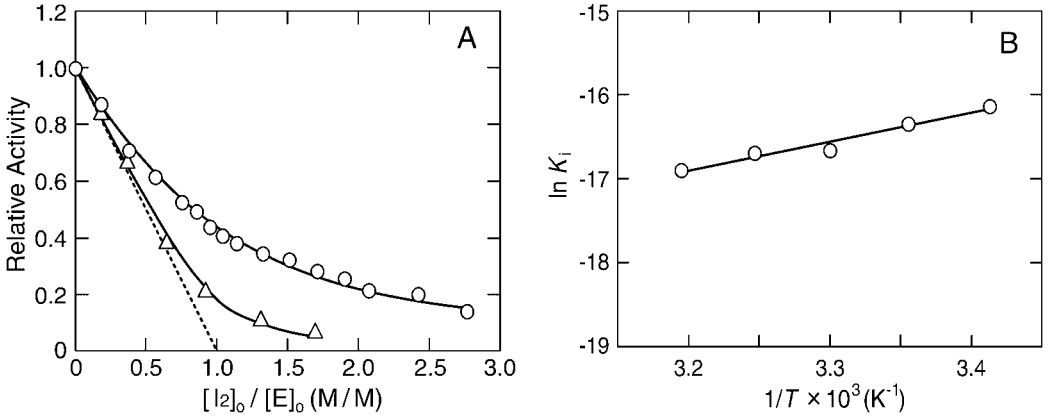

Fig. 4. Inhibitory effect of 0.19 AI on PPA. Panel A: Competitive inhibition of PPA activity by 0.19 AI. The reaction was performed in buffer B containing 25 mM NaCl at 30°C. The initial concentrations of 0.19 AI ($[I_2]_o$) were in the range of 0–457 nM, and that of *p*NP-G2 ($[S]_o$) was 4.0 mM. The initial concentrations of PPA ($[E]_o$) were 165 nM (circles) and 1.32 μM (triangles). The activities of 4.4 and 36.4 nM/s were taken as relative activities of 1.0 at the $[E]_o$ of 165 nM and 1.32 μM, respectively. The inhibitor constant (K_i) was determined to be 57.3 ± 2.7 nM. Panel B: Van't Hoff plots of K_i. The standard enthalpy change ($\Delta H^{\circ\prime}$) for the binding of PPA with 0.19 AI was determined to be 28.2 ± 3.6 kJ mol^{-1}.

with the same slope was obtained in the presence of 117 nM 0.19 AI, and the k_{cat} and K_m values were determined to be (5.25 ± 0.21) × 10^{-2} s^{-1} and 8.93 ± 0.55 mM, respectively. These data indicated that 0.19 AI inhibited PPA activity through an increase in K_m, and the inhibition was judged to be competitive.

Determination of the Inhibitor Constant—Based on the result that 0.19 AI dimer inhibits PPA competitively at a molar ratio of 1:1, the inhibitor constant (K_i) is defined as:

$$K_i = \frac{[E][I_2]}{[EI_2]} \quad (6)$$

where [E], [I_2], and [EI_2] are the concentrations of free PPA, 0.19 AI dimer, and the EI_2 complex, respectively. A relative activity (v/v_o) can be described as:

$$\frac{v}{v_o} = ([E]_o - [I_2]_o - K_i) + \frac{\sqrt{([E]_o - [I_2]_o - K_i)^2 + 4[E]_o[K_i]_o}}{2[E]_o} \quad (7)$$

where $[E]_o$ and $[I_2]_o$ are the initial concentrations of PPA and 0.19 AI dimer, respectively. The effect of 0.19 AI concentration on the relative PPA activity at two different PPA concentrations is shown in Fig. 4A. The K_i value at pH 6.9, 30°C was determined to be 57.3 ± 2.7 nM from Eq. 7 using non-linear least-squares regression (*26*). The degree of inhibition by 0.19 AI depended on the initial PPA concentration in this concentration range, and the result obtained at high PPA concentration also indicated that PPA bound with 0.19 AI dimer (I_2) at a molar ratio of 1:1.

Temperature-dependence of K_i was also examined at pH 6.9, in the temperature range of 20–40°C (Fig. 4B). From the slope of the Van't Hoff plots, the standard enthalpy change ($\Delta H^{\circ\prime}$) for the binding of PPA with 0.19 AI was determined to be 28.2 ± 3.6 kJ mol^{-1}. The standard Gibbs energy change ($\Delta G^{\circ\prime}$) and the standard entropy change ($\Delta S^{\circ\prime}$) for the formation of the EI_2 complex were determined to be –42.0 ± 0.1 kJ mol^{-1} and 232 ± 12 J mol^{-1} K^{-1}, respectively.

Thermal Inactivation of 0.19 AI—Thermal inactivation of 0.19 AI was observed at pH 6.9 in the temperature range of 50–90°C (Fig. 5A). PPA activity was measured at 30°C in the presence of the heat-treated 0.19 AI and found to increase with the increase in incubation time of 0.19 AI. The concentration of active 0.19 AI was calculated from the residual inhibitory activity using Eq. 7 with the K_i value of 57.3 nM. The inactivation followed pseudo-first-order kinetics, and the first-order rate constants, k, at 50, 60, 70, 80, and 90°C were determined to be (1.17 ± 0.06) × 10^{-5}, (3.42 ± 0.07) × 10^{-5}, (9.04 ± 0.02) × 10^{-5}, (1.97 ± 0.03) × 10^{-4}, and (4.18 ± 0.06) × 10^{-4} s^{-1}, respectively. Arrhenius plots of k for the thermal inactivation of 0.19 AI are shown in Fig. 5B. The activation energy for the thermal inactivation was determined to be 87.0 ± 2.4 kJ mol^{-1} from the slope, and the temperature, T_{50}, giving 50% inactivation in a 30-min incubation was determined to be 88.1°C. Eyring plots are also shown in Fig. 5C, and the enthalpy of activation ($\Delta H^{\ddagger}$) and the entropy of activation ($\Delta S^{\ddagger}$) for the inactivation were determined to be 84.2 ± 2.4 kJ mol^{-1} and –78.8 ± 7.0 J mol^{-1} K^{-1}, respectively. The Gibbs energy of activation ($\Delta G^{\ddagger}$) at 50°C and 90°C was calculated to be 110 ± 5 and 113 ± 5 kJ mol^{-1}, respectively.

DISCUSSION

Purification of 0.19 AI—Wheat contains a large number of AIs, many of which have almost the same molecular weight and similar properties. They have been most clearly separated by reversed-phase HPLC at a fairly high temperature, 50°C (*2*). In this study, the purification of the major component of wheat AIs, 0.19 AI, was examined under milder conditions, and 0.19 AI was successfully purified using an anion-exchange HPLC column, TSKgel BioAssist Q. This method could be suitable for the large-scale purification of wheat AIs.

Thermal Inactivation of 0.19 AI—The T_{50} value (88.1°C) of the thermal inactivation of 0.19 AI (Fig. 5) indicates that 0.19 AI is stable against heat treatment,

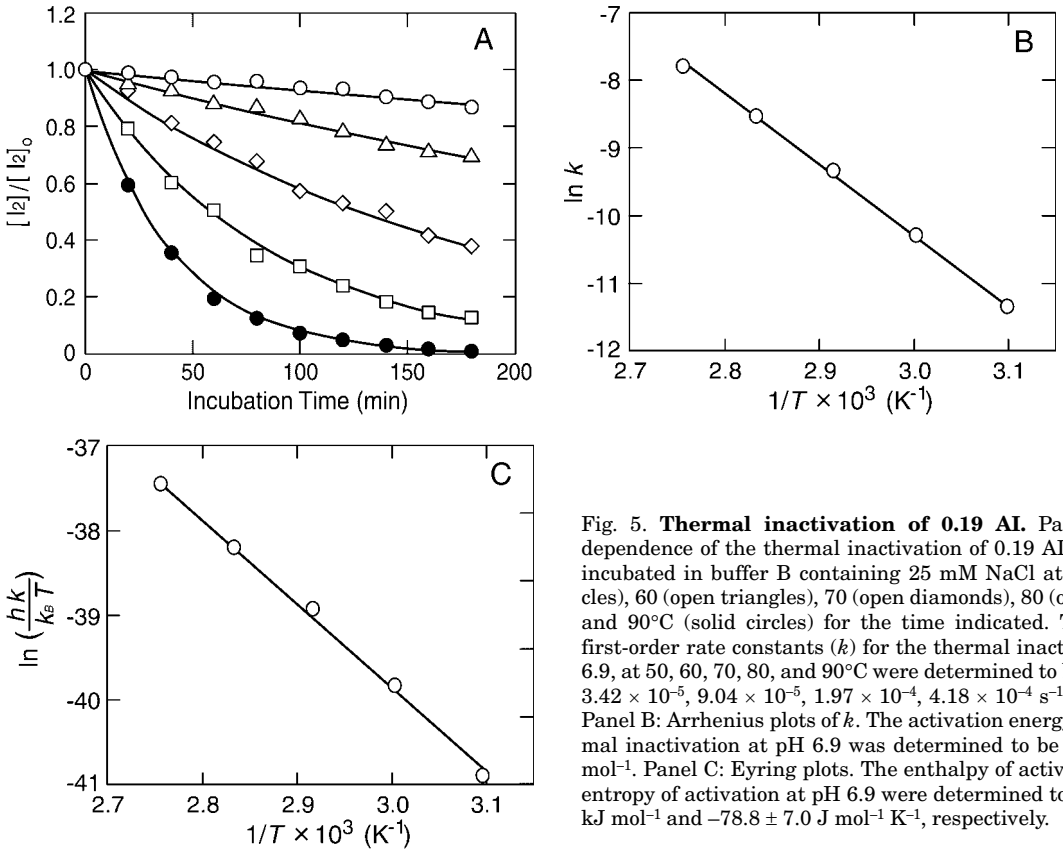

Fig. 5. **Thermal inactivation of 0.19 AI.** Panel A: Time-dependence of the thermal inactivation of 0.19 AI. 0.19 AI was incubated in buffer B containing 25 mM NaCl at 50 (open circles), 60 (open triangles), 70 (open diamonds), 80 (open squares), and 90°C (solid circles) for the time indicated. The apparent first-order rate constants (k) for the thermal inactivation at pH 6.9, at 50, 60, 70, 80, and 90°C were determined to be 1.17×10^{-5}, 3.42×10^{-5}, 9.04×10^{-5}, 1.97×10^{-4}, 4.18×10^{-4} s^{-1}, respectively. Panel B: Arrhenius plots of k. The activation energy for the thermal inactivation at pH 6.9 was determined to be 87.0 ± 2.4 kJ mol^{-1}. Panel C: Eyring plots. The enthalpy of activation and the entropy of activation at pH 6.9 were determined to be 84.2 ± 2.4 kJ mol^{-1} and –78.8 ± 7.0 J mol^{-1} K^{-1}, respectively.

and this value is in reasonable agreement with the T_m value of 93°C reported by differential scanning calorimetric studies (*19*). However, it should be noted that the E_a value (87.0 ± 2.4 kJ mol–1) of the thermal inactivation is considerably lower than those of other proteins, although the T_{50} value is high (*27–29*). The other activation parameters, $\Delta G^{\ddagger}$ of 110–113 kJ mol^{-1}, $\Delta H^{\ddagger}$ of 84.2 kJ mol^{-1}, and $\Delta S^{\ddagger}$ of –78.8 J mol^{-1} K^{-1}, suggest that the activation process of the inactivation of 0.19 AI is endothermic and shifts the 0.19 AI molecule to a more energy-rich and highly-ordered state.

HPLC Analysis of the Complex Formation—Gel-filtration HPLC was performed on TSKgel G2000SW_{XL} equilibrated with 20 mM sodium phosphate buffer (buffer B) containing 0.3 M NaCl to minimize non-specific interactions of proteins with chromatographic gels (*30*). However, PPA (E) and EI_2 complex eluted at the positions corresponding to 17.0 and 35.0 kDa, although their theoretical molecular masses are 55.4 and 82.0 kDa, respectively. On the other hand, 0.19 AI (I_2, 26.6 kDa) was eluted at the position corresponding to 24.0 kDa, suggesting that I_2 is eluted at almost the theoretical position in the gel-filtration HPLC. The discrepancy between the theoretical molecular masses and those evaluated from the elution positions of E and EI_2 suggest non-specific interaction between PPA and the matrix of TSKgel G3000SW_{XL}. Similar behaviors are observed in gel-filtration chromatography of α-amylases from *Bacillus subtilis* (*10*) and *Bacillus licheniformis* (Inouye, K. unpublished data). Although the estimated molecular masses of E and EI_2 are inaccurate, E, I_2, and EI_2 were nevertheless clearly separated, and the binding ratio was determined to be 1:1. When equal amounts of E and I_2, were incubated, a small amount of I_2 was observed in the HPLC, suggesting that the inhibitor constant was in the order of 10^{-8} M (Fig. 2).

Inhibition of PPA Activity by 0.19 AI—Hanes-Woolf plots for the PPA-catalyzed hydrolysis of *p*NP-G2 show the competitive inhibition of PPA activity by 0.19 AI (Fig. 3), and this indicates that 0.19 AI may bind to the substrate-binding site of PPA. The inhibition curves obtained with two different PPA concentrations indicated a K_i value of 57.3 nM and also confirmed the binding ratio of $E:I_2$ = 1:1 (mol/mol) (Fig. 4A). Both HPLC and kinetic analyses indicated the binding ratio of 1:1 (mol/mol), although 0.19 AI is a homodimer composed of two identical subunits. Similar results have been reported in the interaction of 0.19 AI with α-amylases from yellow mealworm (*11*) and chicken pancreas (*13*) by kinetic, difference spectral, gel-filtration and differential scanning calorimetric studies. The K_i values for these α-amylases have been reported to be 0.85 nM at pH 5.3 and 37°C and 3.7 nM at pH 5.8 and 37°C, respectively. On the other hand, the α-amylase inhibitor 0.28 AI, which is a monomer protein similar to the subunit of 0.19 AI in molecular weight and amino acid sequence (*14*, *18*), has been reported to bind these α-amylases at a molar ratio of E:I = 1:2 (*11*, *13*). It is suggested that α-amylases have at least two binding sites for 0.28 AI. These lines of evidence suggest the following explanation for the binding ratio of PPA to 0.19 AI. The PPA molecule has two inhibitor-binding sites. When the primary site is occupied by a 0.19 AI

molecule (I_2), a second I_2 molecule cannot bind to the second site, probably because of the bulkiness of the inhibitor. In the same way, when one of the subunits of 0.19 AI binds PPA, the other subunit cannot bind a second PPA molecule, probably because of the bulkiness of the PPA molecule. We have found that 0.19 AI inhibits PPA competitively, suggesting that the primary inhibitor-binding site on PPA is at the active site and the secondary one might be far from the active site. If a monomer form of 0.19 AI (I) could be prepared by modifying the subunit-interacting area, it is possible that a ternary complex (IEI) might be formed. The structural and functional relationship between the two inhibitor-binding sites on PPA is of great interest.

Thermodynamic analysis has demonstrated that the binding of PPA with 0.19 AI is endothermic and gives a large positive $\Delta S^{\circ\prime}$, indicating that the binding is driven by a large increase in entropy. Unfortunately, the PPA-binding site on 0.19 AI has not yet been identified, but this large increase in entropy suggests that hydrophobic interaction may play a significant role in the binding of PPA with 0.19 AI. An X-ray crystallographic study of the PPA-0.19 AI complex is currently under way. The significance of the dimer structure of 0.19 AI is not known. Recently, we have evaluated the subunit-exchange rate of bovine erythrocyte superoxide dismutase (BESOD) composed of two identical 16-kDa subunits and estimated the physicochemical nature of the subunit interaction (*31*). It is suggested that if the subunit-exchange rate for 0.19 AI could be determined, the kinetic and thermodynamic information for the subunit interaction could be obtained.

Certain α-amylase inhibitors have been shown to have adverse effects on nutrition due to their inhibition of digestive amylase enzymes. On the other hand, the inhibition has been proposed for application in obesity and diabetes (*32*). Naturally occurring proteinaceous α-amylase inhibitors are classified into seven types according to similarities in sequence and three-dimensional structures (*1*, *32*). Their K_i values are in the range of 10^{-6}–10^{-12} M, and the K_i value of 0.19 AI against PPA is almost comparable to the values of the strongest inhibitors. Their thermal stability and physicochemical properties are not known. Synthetic and low-molecular-weight inhibitors, such as acarbose and glucopyranosylidene-spiro-thiohydantoin, have also been extensively studied, but some demerits for therapeutic use have been reported (*33*, *34*). We have demonstrated in this paper the high thermal stability of 0.19 AI as well as its high inhibitory activity against PPA. These observations suggest that 0.19 AI has potential for use in the prevention and therapy of obesity and diabetes.

REFERENCES

1. Franco, O.L., Rigden, D.J., Melo, F.R., and Grossi-de-Sá, M.F. (2002) Plant α-amylase inhibitors and their interaction with insect α-amylases: Structure, function and potential for crop protection. *Eur. J. Biochem.* **269**, 397–412
2. Choudhury, A., Maeda, K., Murayama, R., and DiMagno, E.P. (1996) Character of a wheat amylase inhibitor preparation and effects on fasting human pancreaticobiliary secretions and hormones. *Gastroenterology* **111**, 1313–1320
3. Koide, D., Yamadera, K., and DiMagno, E.P. (1995) Effect of a wheat amylase inhibitor on canine carbohydrate digestion, gastrointestinal function, and pancreatic growth. *Gastroenterology* **108**, 1221–1229
4. Lankisch, M., Layer, P., Rizza, R.A., and DiMagno, E.P. (1988) Acute postprandial gastrointestinal and metabolic effects of wheat amylase inhibitor (WAI) in normal, obese, and diabetic humans. *Pancreas* **17**, 176–181
5. Deponte, R., Parlamenti, R., Petrucci, T., Silano, V., and Tomassi, M. (1976) Albumin α-amylase inhibitor families from wheat flour. *Cereal Chem.* **53**, 805–819
6. Garcia-Maroto, F., Maraña, C., Mena, M., Garcia-Olmedo, F., and Carbonero, P. (1990) Cloning of cDNA and chromosomal location of genes encoding the three types of subunits of the wheat tetrameric inhibitor of insect α-amylase. *Plant Mol. Biol.* **14**, 845–853
7. Sodini, G., Silano, V., De Agazio, M., Pocchiari, F., Tentori, L., and Vivaldi, G. (1970) Purification and properties of a *Triticum aestivum* specific albumin. *Phytochemistry* **9**, 1167–1172
8. Cantagalli, P., Di Giorgio, G., Morisi, G., Pocchiari, F., and Silano, V. (1971) Purification and properties of three albumins from *Triticum aestivum* seeds. *J. Sci. Food Agric.* **22**, 256–259
9. Kashlan, N. and Richardson, M. (1981) The complete amino acid sequence of a major wheat protein inhibitor of α-amylase. *Phytochemistry* **20**, 1781–1784
10. Takase, K. (1994) Site-directed mutagenesis reveals critical importance of the catalytic site in the binding of α-amylase by wheat proteinaceous inhibitor. *Biochemistry* **33**, 7925–7930
11. Buonocore, V., Gramenzi, F., Race, W., Petrucci, T., and Poerio, E. (1980) Interaction of wheat monomeric and dimeric protein inhibitors with α-amylase from yellow mealworm (*Tenebrio molitor* L. Larva). *Biochem. J.* **187**, 637–645
12. Franco, O.L., Rigden, D.J., Melo, F.R., Bloch, Jr, C., Silva, C.P., Grossi, de Sá, M.F. (2000) Activity of wheat α-amylase inhibitors towards bruchid α-amylases and structural explanation of observed specificities. *Eur. J. Biochem.* **267**, 2166–2173
13. Buonocore, V., Giardina, P., Parlamenti, R., Poerio, E., and Silano, V. (1984) Characterization of chicken pancreas α-amylase isomers and interaction with protein inhibitors from wheat kernel. *J. Sci. Food Agric.* **35**, 225–232
14. Petrucci, T., Rab, A., Tomasi, M., and Silano, V. (1976) Further characterization studies of the α-amylase protein inhibitor of gel electrophoretic mobility 0.19 from wheat kernel. *Biochim. Biophys. Acta* **420**, 288–297
15. Maeda, K., Kakabayashi, S., and Matubara, H. (1985) Complete amino acid sequence of an α-amylase inhibitor in wheat kernel (0.19-inhibitor). *Biochim. Biophys. Acta* **828**, 213–221
16. Oda, Y., Matunaga, T., Fukuyama, K., Miyazaki, T., and Morimoto, T. (1997) Tertiary and quaternary structure of 0.19 α-amylase inhibitor from wheat kernel determined by X-ray analysis at 2.06 Å resolution. *Biochemistry* **36**, 13503–13511
17. Silano, V., Pocchiari, F., and Kasarda, D.D. (1973) Physical characterization of α-amylase inhibitors from wheat. *Biochim. Biophys. Acta* **317**, 139–148
18. Petrucci, T., Sannia, G., Roberto, P., and Silano, V. (1978) Structural studies of wheat monomeric and dimeric protein inhibitors of α-amylase. *Biochem. J.* **173**, 229–235
19. Silano, V. and Zahnley, J.C. (1978) Association of *Tenebrio molitor* L. α-amylase with two protein inhibitors – one monomeric, one dimeric – from wheat flour. *Biochim. Biophys. Acta* **533**, 181–185
20. Darnis, S., Juge, N., Guo, X.-J., Marchis-Mouren, G., Puigserver, A., Chaix, J.-C. (1999) Molecular cloning and primary structure analysis of porcine pancreas α-amylase. *Biochim. Biophys. Acta* **1430**, 281–289
21. Laemmli, U.K. (1970) Cleavage of structural proteins during the assembly of the head of bacteriophage T4. *Nature* **227**, 680–685
22. Levitzki, A. and Steer, M.L. (1974) The allosteric activation of mammalian alpha-amylase by chloride. *Eur. J. Biochem.* **41**, 171–180
23. Yamashita, H., Nakatani, H., and Tonomura, B. (1991) Substrate-selective activation of histidine-modified porcine pancreas α-amylase by chloride ion. *J. Biochem.* **110**, 605–607

24. Segel, I.H. (1975) *Enzyme Kinetics*, pp. 926–942, John Wiley and Sons, New York
25. Laidler, K.J., and Meiser, J.H. (1999) Physical Chemistry, 3rd ed., pp. 369–419, Houghton Mifflin Company, Boston, MA
26. Sakoda, M. and Hiromi, K. (1976) Determination of the best-fit values of kinetic parameters of the Michaelis-Menten equation by the method of least squares with Taylor expansion. *J. Biochem.* **80**, 547–555
27. Inouye, K., Osaki, A., and Tonomura, B. (1994) Dissosiation of dimer of bovine erythrocyte Cu, Zn-superoxide dismutase and activity of the monomer subunit: Effects of urea, temperature, and enzyme concentration. *J. Biochem.* **115**, 507–515
28. Inouye, K., Kuzuya, K., and Tonomura, B. (1998) Sodium chloride enhances markedly the thermal stability of thermolysin as well as its catalytic activity. *Biochim. Biophys. Acta* **1388**, 209–214
29. Inouye, K., Tanaka, H., and Oneda, H. (2000) States of tryptophyl residues and stability of recombinant human matrix metalloproteinase 7 (matrilysin) as examined by fluorescence. *J. Biochem.* **128**, 363–369
30. Inouye, K. (1991) Chromatographic behaviors of proteins and amino acids on a gel filtration matrix, TSK-gel Toyopearl. *Agric. Biol. Chem.* **55**, 2129–2139
31. Oneda, H. and Inouye, K. (2003) Effect of nitration on the activity of bovine erythrocyte Cu, Zn-superoxide dismutase (BESOD) and a kinetic analysis of its dimerization-dissociation reaction as examined by subunit exchange between the native and nitrated BESODs. *J. Biochem.* **134**, 683–690
32. Svensson, B., Fukuda, K., Nielsen, P.K., and Bonsager, B.C. (2003) Proteinaceous α-amylase inhibitors. *Biochim. Biophys. Acta*, in press
33. Truscheit, E., Frommer, W., Junge, B., Mueller, L., Schmidt, D.D., and Wingender, W. (1981) Chemistry and biochemistry of microbial α-glucosidase inhibitors. *Angew. Chem.* **93**, 738–755
34. Gyemant, G., Kandra, L., Nagy, V., and Somasak, L. (2003) Inhibition of human salivary a-amylase by glucopyranosylidene-spiro-thiohydantoin. *Biochem. Biophys. Res. Commun.* **312**, 334–339